American Mineralogist, Volume 84, pages 913–921, 1999

Crystal structure of non-metamict Th-rich hellandite-(Ce) from Latium (Italy) and crystal chemistry of the hellandite-group minerals

ROBERTA OBERTI,[1,*] LUISA OTTOLINI,[1] FERNANDO CAMARA,[1,†] AND GIANCARLO DELLA VENTURA[2]

[1]CNR-CS per la Cristallochimica e la Cristallografia, via Ferrata 1, I-27100 Pavia
[2]Dipartimento Scienze Geologiche, Università di Roma Tre, largo S. Leonardo Murialdo 1, I-00146 Roma

ABSTRACT

The crystal structure of a Th-U-rich, Y-poor hellandite-(Ce) occurring in a volcanic ejectum from Capranica (Vico volcanic complex, Latium, Italy) was refined to an R index of 1.5% for 2226 observed reflections [$I > 3\ \sigma(I)$]. Hellandite from Capranica is monoclinic $P2/a$ with a = 19.068 (8), b = 4.745 (2), c = 10.289 (3) Å, β = 111.18 (3)°. The extra-framework (distorted) tetrahedral cavity, usually occupied by H in hellandite, is partially (35–40%) occupied by Be and/or Li. When this is the case, the $[B_4Si_4O_{22}]$ tetrahedral chains of hellandite are locally cross-linked to form a sheet, which is built up by the same types of rings as in semenovite but in a different arrangement. The structure refinement and the electron- and ion-microprobe analyses provide constraints on hellandite-group crystal chemistry. The presence of $^{[4]}$(Be, Li) at the Be site is coupled with the substitution of F and/or O for OH at the O5 site; the amount of extra-framework cations thus constrains the OH content in the general formula. X-ray data exclude the presence of other OH sites in the structure, in agreement with direct H determination by ion probe (1.02 H apfu + 0.98 F apfu = 2.0 apfu of monovalent anions at O5 vs. 4.5–8 apfu proposed previously). The complete chemical analysis also eliminates the need for a vacancy at the REE sites. The general formula of hellandite-group minerals is thus $(Ca,REE)_8(Th,U,Y,REE)_4(Ti,Fe^{3+},Al)_2(O,F,OH_x)_4(Be,Li)_{4-x}Si_8B_8O_{44}$, where electroneutrality is assured by the appropriate mixing of heterovalent substituents at the M sites.

INTRODUCTION

Hellandite is a rare, Y-bearing borosilicate, typically associated with granitic rocks or granitic pegmatites. The structure of hellandite was determined by Mellini and Merlino (1977) on a specimen from Predazzo, Italy and described as $[B_4Si_4O_{22}]$ chains parallel to the c axis, which are cross-linked into a framework by sharing vertices with (Al, Fe^{3+}) M1 octahedra (Fig. 1). This structural arrangement results in tunnels extending along the c axis, which are filled by a combination of three distinct distorted eightfold-coordinated sites (M2, M3, and M4) occupied by Ca, Y, REE, actinides and possibly vacancies (□). Y is considered proxy for HREE because of similarities in the ionic size and geochemical behavior. Samples from Predazzo have a non-homogeneous distribution between Ca and lanthanides, with a strong preference of (Y + REE) at M2 >> M4 > M3 (Mellini and Merlino 1977). At that time, accurate determination of all the chemical constituents, in particular the light elements H and B, was not possible. Therefore, the B content was calculated on the basis of the structure refinement to give 8 atoms per formula unit (apfu) and the water content was calculated to give 48 O atoms apfu. With this procedure, significant vacancies (1.5 apfu) at the (M2–M4) sites were obtained, and the crystal-chemical formula was proposed to be $[Ca_{5.5}(Y,REE)_{5.0}\square_{1.5}](Al_{1.1}Fe^{3+}_{0.9})(OH)_4[Si_8B_8O_{40}(OH)_4]$. Bond-valence calculations showed that four of these eight OH groups occupied the O5 anionic site; this inference was also supported by a residual at the appropriate position in the difference Fourier map calculated at convergence. Bond-valence calculations also showed that the other four H atoms pfu were bonded (with 0.5 occupancy) to the O6 and O7 atoms. Analyses of other hellandites from Wakefield Lake, Canada, (Hogarth et al. 1972) and Kragerö, Norway, (Oftedal 1965) gave even higher water contents than the Predazzo sample, suggesting the presence of additional OH groups in the structure (Mellini and Merlino 1977).

Three new occurrences of hellandite were recently described: Quyang, Hebei, China (Ma et al. 1986), Tahra, Japan (Miyawaki et al. 1987), and Mattagami Lake, Canada (Pan et al. 1994). The proposed formulas are respectively $[(Ca_{4.32}Na_{0.06}K_{0.16}Fe^{2+}_{0.18}Mn_{0.10}Y_{4.06}La_{0.06}Ce_{0.28}Pr_{0.04}Nd_{0.20}Sm_{0.10}Gd_{0.20}Tb_{0.06}Dy_{0.36}Ho_{0.10}Er_{0.24}Tm_{0.04}Yb_{0.22}Lu_{0.02}Sc_{0.04})Al_{1.68}Fe^{3+}_{0.74}Be_{1.18}B_{6.72}Si_{8.82}O_{40}(OH)_{8.92}]$, $[(Ca_{5.75}Y_{3.70}Nd_{0.24}Dy_{0.21}Gd_{0.16}Yb_{0.15}Ce_{0.13}Er_{0.13}Sm_{0.12}Ho_{0.06})(Al_{1.45}Mn_{0.25}Ti_{0.21}Fe_{0.11})Si_8B_8O_{40.22}(OH)_{7.78}]$ both of which were taken from Anovitz and Hemingway (1996) and $[(Ca_{5.15}Y_{3.91}Nd_{0.01}Sm_{0.03}Eu_{0.05}Gd_{0.27}Dy_{0.49}Er_{0.26}Yb_{0.14})(Al_{1.81}Fe^{2+}_{0.21}Mg_{0.30}Zn_{0.08})B_{7.97}Si_{8.00}O_{40}(OH)_{7.81}]$ which was recalculated according to the structural formula of Mellini and Merlino (1977).

An anhydrous phase, tadzhikite, with the formula $Ca_6(Ce,Nd,La,\square)_6(Ti,Fe,Al)_2(Si,Be)_8B_8O_{46}$, which is mono-

*E-mail: oberti@crystal.unipv.it
†Present address: Geology Department, Arizona State University, Tempe, Arizona 85827-1404, U.S.A.

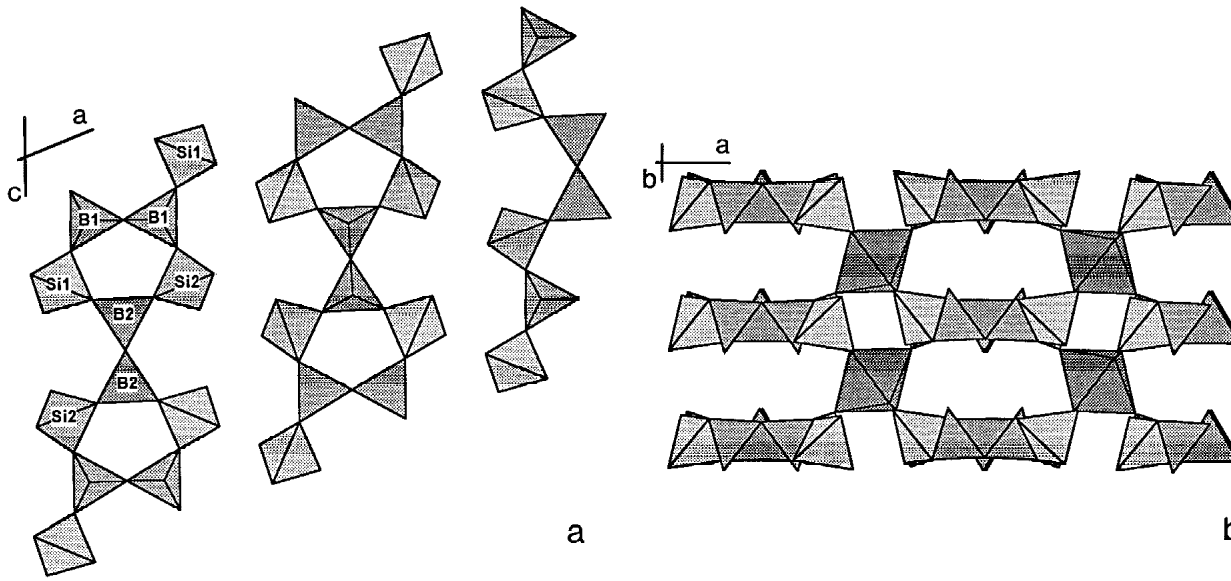

FIGURE 1. The structure of hellandite projected along [010] **(a)** and along [001] **(b)**. Tetrahedra with B are more darkly shaded than those with Si. Moctahedra have the darkest shading.

clinic with $a = 17.93$, $b = 4.71$, $c = 10.39$ Å, and $\beta = 100.27°$, was proposed to be the anhydrous Ti, Ce-analogue of hellandite (Yefimov et al. 1970). However, Mellini and Merlino (1977) pointed out that the unit-cell parameters of tadzhikite could be transformed into those of hellandite simply by taking the diagonal between **a** and **c** as the *a* edge and inverting the direction of *c* edge. Hellandite and tadzhikite were thus isostructural. The same authors suggested that the difference in chemistry could be ascribed either to analytical problems (F substitution for OH and lack of F detection) or to the presence of high Ti and REE contents balancing for the lack of OH groups. Chernitsova et al. (1982) refined the structure of a partially α-decay damaged tadzhikite with composition $Ca_{6.36}(Y,REE)_{4.4}(Ti_{0.86}Fe_{0.74}Al_{0.62})(Si,Al)_8B_{8.08}O_{44}$ after heating the sample at 700 °C. They concluded that tadzhikite was isomorphous with hellandite and could be considered as the anhydrous (Ti,Ce)-rich member of the hellandite group. In their proposed general formula, $(Ca,REE)_8(Y,REE)_4(Ti,Fe,Al)_2(O,OH)_4Si_8B_8O_{44}$, the charge imbalance due to the absence of H is compensated by Ti^{4+}.

Cooper et al. (1998) refined the structure of tadzhikite before thermal treatment, and found significant positional disorder of the REE at the M2 site. Four subsites were refined within the M2 cavity, and the positional disorder was related to the partially metamict state of their sample. Bond-valence analysis showed that this tadzhikite contained a significant amount of water, and the authors proposed the following structural formula: $Ca_2(Ca,Y)_2(R^{3+},\square)_2(Ti^{4+},Fe^{3+})[B_4Si_4O_{16}(O,OH)_6](OH)_2$. In this formula, the anionic O5 site is occupied by OH, and the other hydroxyls distribute among O1, O3, and O7 because of local (short-range) bond-valence requirements due to a locally vacant M2 site.

Several problems remain concerning the crystal chemistry of the hellandite-group minerals, namely (1) their correct crystal-chemical formula, (2) the number and location of the hydroxyls in the structure, and (3) the relation between hellandite and tadzhikite. These problems are due partly to the metamict state of the samples and partly to common and strong alteration of hellandite (Hogarth et al. 1972). This paper addresses these problems by applying microchemical and X-ray techniques to a non-metamict variety of hellandite rich in Th, U, and LREE and depleted in Y.

EXPERIMENTAL METHODS

Sample description

The hellandite crystals were found inside a volcanic ejectum collected near Capranica (Viterbo Province), north of Rome, within an explosive breccia belonging to one of the pyroclastic flow units (ignimbrite "C") of the Vico volcanic complex (Locardi 1965). The host rock can be classified as an alkali-syenite. It is massive and fine-grained and is composed of abundant alkali-feldspar ($Or_{70}Ab_{30}$), some plagioclase ($Ab_{85}An_{15}$), and minor F-rich biotite, augitic clinopyroxene and (Fe, Mn, Ti)-oxides. Hellandite occurs inside miarolitic cavities resulting from the interlocked texture of the feldspars and is typically associated with vonsenite, helvite, baddeleyite, vicanite, and britholite. Crystals are euhedral, transparent, light-green colored, with a maximum dimension of 0.3–0.4 mm. Hellandite is also observed inside the groundmass of the ejectum; in this case it fills voids and fractures inside the rock and is systematically intergrown with britholite. Details on the mineralogy of the studied ejectum as well as on the complex genetical conditions for the observed mineral associations are given by Della Ventura et al. (unpublished manuscript).

X-ray analysis, data collection, and structure refinement

Several crystals selected for crystallographic analysis based on optical behavior and freedom from inclusions were mounted on a Philips PW-1100 automated four-circle diffractometer and examined with graphite-monochromatized Mo*K*α radiation. Crystal quality was assessed using the profiles and widths of

TABLE 1. Selected crystal and refinement data

a (Å)	19.068 (8)	θ range (°)	2-30
b (Å)	4.745 (2)	No. all	2671
c (Å)	10.289 (3)	No. obs	2226
β (°)	111.18 (3)	R sym (%)	1.2
V (Å^3)	867.9 (6)	R all (%)	2.3
Space group	*P*2/*a*	R obs %	1.5

Bragg diffraction peaks. Unit-cell dimensions were calculated from least-squares refinement of the *d*-values obtained from 60 rows of the reciprocal lattice by measuring the center of gravity of reflections in the θ range between –35 and 35°. Intensity data of the monoclinic equivalent pairs *hkl* and *h*-*kl* were collected using the step-scan profile technique of Lehman and Larsen (1974); integration was made by means of profile-fitting analysis. The data were corrected for absorption following the method of North et al. (1968), for Lorentz and polarization effects, averaged and reduced to structure factors.

The space group of hellandite from Capranica is *P*2/*a*, as reported by Mellini and Merlino (1977). However, some violations of the systematic extinctions for *h*0*l* with $h = 2n + 1$ were observed; their occurrence will be discussed in a following section.

During the structure refinement, fully ionized scattering factors (with terms for the anomalous dispersion) were used for all sites (cationic and anionic) at which isomorphous substitutions were likely to occur and could be evaluated also on the basis of the refined site-scatterings; neutral vs. ionized scattering factors were used for all O atoms except O5, to obtain estimates for their formal charges. Additional details on the refinement procedure are given in Hawthorne et al. (1995a). In particular, we refined Al^{3+} vs. Fe^{3+} at M1, Ca^{2+} vs. Th^{4+} at M2, Ca^{2+} vs. Ce^{3+} at M3, and Ca^{2+} vs. Ce^{3+} at M4, O^{-1} vs. F^{-1} at O5. The tetrahedral sites were first refined with Si vs. Be (Si1, Si2) and B vs. vacancy (B1, B2), resulting in $Z = 14.0$ and 5.0, respectively, and mean bond lengths suitable for single-element occupancy. Therefore, the subsequent cycles were done with ionized vs. neutral scattering factors for Si and with fixed occupancy for B, for which a reliable B^{3+} scattering curve is not available. The structure refinement was done on the reflections with $I > 3\sigma(I)$ starting from the coordinates of Mellini and Merlino (1977) and converged to $R = 2.0\%$. A difference Fourier-map showed a residual maximum (corresponding to 3.9 e/Å^3) at ~1.5 Å from the O3 and O5 atoms. Because preliminary SIMS analyses showed the presence of some Be, which could not be placed in the Si and B tetrahedra because of the refined site-scatterings and mean bond-lengths, a new site was added to the structural model and anisotropically refined by using Be^{2+} vs. vacancy. The *R* factor decreased to 1.6%, and the Be site was found to have a distorted tetrahedral coordination and partial (~0.40) occupancy. At this point, the first residual in the difference Fourier map was at 1.06 Å from O5 (peak height 0.9 e/Å^3), and could be interpreted as H; as it was also at 1.0 Å from the partially occupied Be site, it was inserted in the model with a (fixed) occupancy complementary to that of Be, and only its coordinates were refined in the subsequent cycles. At convergence, the O5-H distance was 0.87 Å and the *R* factor decreased to 1.5%. Unit-cell parameters and selected data-collection and refinement parameters are given in Table 1, atomic coordinates, equivalent isotropic atomic displacement parameters and refined site-scatterings in Table 2, selected interatomic distances in Table 3, observed and calculated structure factors in Tables 4[1], anisotropic components of the atomic displacement parameters in Table 5[1].

TABLE 2. Atomic fractional coordinates, equivalent isotropic atomic displacement parameters (Å^2) and refined site-scattering (ss; epfu)

	ss	*x*/*a*	*y*/*b*	*z*/*c*	B_{eq}
B1	20.00	0.1735(1)	0.5271(6)	0.4518(3)	0.47(6)
B2	20.00	0.2528(1)	0.4618(5)	0.1334(3)	0.40(5)
Si1	56.00	0.1040(1)	0.4838(1)	0.6503(1)	0.37(1)
Si2	56.00	0.1130(1)	0.4980(1)	0.1622(1)	0.47(1)
M1	39.18	0	0	0	0.70(2)
M2	239.16	0.0430(1)	0.0171(1)	0.3609(1)	0.60(1)
M3	84.12	0.2476(1)	0.0028(1)	0.6610(1)	0.64(1)
M4	103.96	0.1567(1)	–0.0333(1)	0.9312(1)	0.75(1)
Be	6.08	0.0373(5)	0.5444(20)	0.8659(10)	1.00(22)
H	2.40	0.0434(30)	0.3712(60)	0.8889(30)	1.00
O1		0.0440(1)	0.2445(4)	0.5675(2)	0.63(4)
O2		0.1787(1)	0.3176(4)	0.7582(2)	0.59(4)
O3		0.0715(1)	–0.3033(4)	0.7365(2)	1.17(5)
O4		0.1330(1)	–0.3339(4)	0.5413(2)	0.65(4)
O5	33.32	0.0370(1)	0.1930(4)	0.8702(2)	0.93(4)
O6		0.2469(1)	–0.2427(4)	0.8585(2)	0.57(4)
O7		0.1682(1)	0.2313(4)	0.4468(2)	0.58(4)
O8		0.1334(1)	0.6717(4)	0.3092(2)	0.78(4)
O9		0.1863(1)	0.3251(4)	0.1583(2)	0.74(4)
O10		0.0847(1)	0.7267(5)	0.0387(2)	1.24(5)
O11		0.0515(1)	0.2578(5)	0.1568(2)	1.25(5)
O12		1/4	0.3368(5)	0	0.72(6)
O13		1/4	0.6483(5)	1/2	0.59(6)

Electron microprobe analyses

After the structure refinement, the crystal was embedded in epoxy-resin and polished. WDS-EMP analyses were done with an ARL microprobe at the Dipartimento di Scienze della Terra (Università di Modena, Italy). Analytical conditions were 15 kV and 20 nA beam current. Natural minerals were used as standards, namely: fluorite (F*K*α), clinopyroxene KH1 (Si*K*α, Ca*K*α), microcline BH1 (K*K*α), ilmenite BH7 (Fe*K*α, Ti*K*α), spessartine BH5 (Mn*K*α), paracelsian Chgo/32 (Ba*L*α). The data were processed with the program PROBE 5.2 (Donovan and Rivers 1990), after Phi-Rho-Z correction following Armstrong (1988).

Ion microprobe analyses

The same crystal was coated with gold (~400 ≈ thickness), bombarded with a $^{16}O^-$ primary beam, and analyzed using a Cameca IMS 4f ion microprobe. Experimental conditions and calibration procedures are as follows.

REE and actinides. Measurements of La, Ce, Pr, Nd, Sm, Eu, Gd, Dy, Er, and Yb were done with 3 nA current intensity focused into a spot of ~5 mm in diameter. The width of the energy slit was 50 eV and the voltage offset applied to the sample accelerating voltage (+4500 V) was –100 V. The methods of energy filtering were similar to those previously developed for silicates (Bottazzi et al. 1994). The main differences in the mass acquisition list concern: (1) the additional detection of $^{141}Pr^+$ secondary ions; (2) shorter counting times for $^{139}La^+$

[1]For a copy of Table 4 or Table 5, document item AM-99-010, contact the Business Offices of the Mineralogical Society of America (see inside fron cover of recent issue) for price information) Deposit items may also be available on the American Mineralogist web site at http://www.minsocam.org.

TABLE 3. Selected interatomic distances (Å) and geometrical describers

B1-O4	×1	1.547	B2-O2	×1	1.538
B1-O7	×1	1.407	B2-O6	×1	1.404
B1-O8	×1	1.549	B2-O9	×1	1.526
B1-O13	×1	1.476	B2-O12	×1	1.478
<B1-O>		1.495	<B2-O>		1.487
V (Å^3)		1.69	*V* (Å^3)		1.67
TAV		40.84	TAV		42.79
TQE		1.010	TQE		1.010
Si1-O1	×1	1.618	Si2-O8	×1	1.641
Si1-O2	×1	1.656	Si2-O9	×1	1.634
Si1-O3	×1	1.609	Si2-10	×1	1.609
Si1-O4	×1	1.662	Si2-11	×1	1.622
<Si1-O>		1.636	<Si2-O>		1.626
V (Å^3)		2.24	*V* (Å^3)		2.20
TAV		5.91	TAV		11.62
TQE		1.002	TQE		1.003
M1-O5	×2	1.950	M2-O1	×1	2.377
M1-O10	×2	1.996	M2-O1	×1	2.393
M1-O11	×2	1.980	M2-O3	×1	2.457
<M1-O>		1.975	M2-O4	×1	2.620
V (Å^3)		10.18	M2-O5	×1	2.521
OAV		21.97	M2-O7	×1	2.447
OQE		1.006	M2-O8	×1	2.570
			M2-O11	×1	2.447
			<M2-O>		2.479
			V (Å^3)		25.87
M3-O2	×1	2.431	M4-O2	×1	2.580
M3-O4	×1	2.626	M4-O3	×1	2.438
M3-O6	×1	2.347	M4-O5	×1	2.392
M3-O7	×1	2.432	M4-O6	×1	2.331
M3-O7	×1	2.504	M4-O6	×1	2.485
M3-O8	×1	2.685	M4-O9	×1	2.778
M3-O9	×1	2.386	M4-O10	×1	2.346
M3-O13	×1	2.373	M4-O12	×1	2.416
<M3-O>		2.473	<M4-O>		2.471
V(Å^3)		25.44	*V* (Å^3)		25.43
Be-O3	×1	1.830	H-O5		0.866
Be-O5	×1	1.668			
Be-O10	×1	1.888			
Be-O11	×1	1.875			
<Be-O>		1.815			

Notes: Esd on distance: 0.002 Å. Distortion parameters are: TAV = tetrahedral angular varience; TQE = tetrahedral quadratic elongation; OAV = octahedral angular varience; OQE = octahedral quadratic elongation.

and $^{140}Ce^+$ isotope (20 s over 10 cycles, respectively), 100 s counting time being used for ^{167}Er, ^{174}Yb in the HREE mass spectrum; (3) selections of Ca (tested as ^{42}Ca as well as ^{44}Ca isotope) as the matrix reference-element; (4) addition of ^{89}Y, ^{232}Th, and ^{238}U isotopes to the secondary-ion-mass-acquisition list; and (5) Ba content was checked at 137 amu.

Standards with uniform, known concentrations of REE and similar major-element composition were used to convert relative ion-intensity to elemental concentrations. Due to the high REE contents of hellandite, we used the REE-enriched Ca-Al-Si-glasses prepared by Drake and Weill (D&W) (1972), which contain different combinations of four REE (and Y) oxides at concentrations ~4 wt% each, CaO and SiO_2 contents being ~26 wt% and 27 wt%, respectively; moreover, we preferred to use Ca as the internal reference-element because it is less sensitive than Si to matrix and machine effects (Hinton 1990; CNR-CSCC unpublished results).

The D&W glasses also allow for calibration of 3 or 4 REE in turn without the interferences from other REE of the mass spectrum. These interferences in the secondary ion spectrum are often dramatic: in allanite, LRE monoxide peaks are of comparable intensity to HRE peaks, causing severe overlapping between the signals (Reed 1985). Our analytical procedure allowed us to remove most of complex molecular interferences and to deconvolute interferences acting on Gd isotopes, mainly associated to NdO^+ and CeO^+ contributions.

The ion yields for REE relative-to-calcium, IY(REE/Ca), defined as the REE-to-calcium intensity ratio relative to the corresponding elemental atomic concentration ratio, are representative of their ionization behavior and allow ion signals to be converted into elemental concentrations. Those derived from D&W glasses were checked against NIST-610 glass (72 wt% SiO_2; 14 wt% CaO; REE and Y concentrations ~500 ppm each), on an inter-laboratory sample (basaltic glass BB) and on an international standard (Snarum apatite). The agreement among the IYs for REE and Y was always better than 15%, typically within 10%, for all the standards used in the comparison, which represents in most cases the estimated uncertainty on the assumed reference concentrations. On this basis, no specific matrix-effect, related to chemical composition, was detected.

Several inter-laboratory samples were also tested under the same experimental conditions to accurately estimate U/Ca and Th/Ca ratios. The agreement between their ion yields was ~10% (15% with NIST-610). The distribution of U and Th in hellandite from Capranica is not homogeneous; analyses carried out under the same experimental conditions with an accurate control of current intensity and focusing of the primary beam gave ThO_2 in the range 7.22–10.63 wt% and UO_2 = 1.07–1.64 wt%, thus suggesting compositional zoning. In-situ SIMS analyses also evidenced a linear inverse relationship between LREE and actinides, which was confirmed by very subtle changes in the Z-contrast grey-levels in high-resolution BSE images (Della Ventura et al., unpublished manuscript).

Light elements. Li, Be, and B were analyzed according to the procedure developed for silicates by Ottolini et al. (1993), which involves energy-filtering methods and working curves to convert ion signals to corresponding elemental concentrations. NIST-610, Ceran, Macusani rhyolite, danalite, and Pyrex glass were used as standards; in the case of Li, the data were further corrected for the low silica content of hellandite, thus calibrating the residual matrix effects still acting on Li ionization. The accuracy of the SIMS analyses for B was shown to be better than ±3% for B (Hawthorne et al. 1995b) and ±5% for Li (CNR-CSCC, unpublished results).

SIMS analysis of H signal in such a matrix was not straightforward due to the lack of standards suitable for H quantification in REE-enriched samples. H ionization is known to suffer from matrix effects, mainly related to Si (and Fe) contents, but there are no data for REE-enriched minerals. The available method for SIMS analysis of H (Ottolini et al. 1995) involves long degassing time in the sample chamber, background correction for H and the use of different calibration curves for different Si contents of the matrix. In the present work, a calibration curve H^+/Si^+ vs. H(at%)/Si(at%) [where H^+ and Si^+ are the secondary ion signals and H(at%) and Si(at%) their respective atomic percent concentrations] was built with three inter-laboratory basaltic glasses; from this, an IY(H/Si) was derived. To reduce possible residual matrix effects on H ionization, re-

lated at a first approximation to the different silica contents between the standards and the "unknown," we also calculated the IY of Ca with respect to Si in all these matrices. The investigation of Ca/Si ionization allowed us to obtain the most reliable IY(H/Ca) for hellandite, which was then used to convert H^+/Ca^+ secondary ion intensities into H_2O wt% concentration. Even if the accuracy of this procedure cannot be exactly stated due to the lack of an hellandite standard for H, we believe that the matrix effects have been reasonably well calibrated.

Fluorine was added to the acquisition list because this element is crucial in the definition of the stoichiometry of hellandite. The procedure developed by Ottolini et al. (1994) on silicates was followed, which relies on the use of a calibration curve against Si built with several reference standards; we used topaz. The agreement within F analyses with SIMS and with structure refinement is 26% and with SIMS and EMPA is 16%.

RESULTS AND DISCUSSION

Chemical composition and REE patterns

The complete chemical analysis of hellandite from Capranica (Table 6) was obtained by combining the SIMS data for the low-Z (H, Li, Be, B, and F) and high-Z (Y, REE, Th, and U) elements with the EMP data for the intermediate-Z elements. The unit-formula was calculated on the basis of 48 (O + F). Site distribution was made on the basis of the refinement results, as discussed below. Site scatterings calculated from this formula compare well with those obtained from the structure refinement: 5.4 vs. 6.1 epfu at the extra-framework tetrahedral site, 38.8 vs. 39.2 epfu at M1, 409.1 vs. 427.2 epfu at the M2–M4 sites, 33.0 vs. 33.3 epfu at O5. The excellent agreement (relative difference = 1.0, 4.2, and 0.9%, respectively) obtained for the fully occupied sites by the two independent approaches is evidence of the accuracy of both techniques.

Hellandite from Capranica significantly differs in chemistry from all other samples so far reported. It is strongly depleted in Y, an essential constituent of hellandite, and has higher Ca, Th, U, and REE. The chondrite-normalized REE pattern [REEcn, averaged on four analyses, normalization-factors C1 from Anders and Ebihara (1982)] in Figure 2 shows that hellandite from Capranica is characterized by an enrichment in the LREEs (La_N/Yb_N = 22.61), and exhibits a linear decrease in REE contents from La towards the HREEs with a negative Eu anomaly (Eu/Eu* = 0.37).

Hellandite has been reported in (1) granite pegmatites [Kragerö, Norway, Brögger 1922; Hogarth et al. 1972, Mellini and Merlino 1977; Wakefield Lake, Quebec, Hogarth et al. 1972]; (2) granite (Predazzo, Italy: Emiliani and Gandolfi 1965); (3) pegmatites (Quyang, China, Ma et al. 1986; Tahra, Japan; Miyawaki et al. 1987); as major constituent in (4) aegirine, quartz, microcline pegmatoid veins cutting alkalic aegirine syenite in the Alay alkalic province, Tadzhikistan (Yefimov et al. 1970; Chernitsova et al 1982; Cooper et al. 1998); and (5) cross-cutting microveins of quartz, sphalerite and chlorite in the chloritite footwall zone at Mattagami Lake deposit (Pan et al. 1994). Hellandite from Mattagami Lake shows a REE distribution characterized by a marked enrichment in the MREE (particularly Gd and Dy), with a concave-downward REEcn pattern devoid of a Eu-anomaly (Fig. 2); this is consistent with its crystallization within a vein with the paragenesis described above. Hellandite from Kragerö shows significant HREE-enrichment but a pronounced Eu-anomaly. Tadzhikite from Alay shows a moderately LREE-enriched chondrite-normalized pattern (La_N/Yb_N = 6.17). Hellandites from pegmatites (Quyang and Tahra) show substantially flat REEcn patterns, slightly depleted in LREE. Besides the Eu anomaly, which is known to be chiefly controlled by coexisting feldspars, the patterns of Figure 2 suggest that the hellandite structure does not show any selectivity towards incorporation of REE, their proportions being probably ruled mainly by the paragenesis and the geological history of the rock. For this reason, hellandite can be used to monitor the fluid composition in the geological environment of formation, provided reasonably constant *P* and *T* conditions.

The tetrahedral framework

Both X-ray single-crystal refinement and microchemical results are consistent with 8 Si and 8 B apfu at the tetrahedral sites. However, SIMS analysis shows significant Be (0.98 apfu) in hellandite from Capranica and a difference Fourier-map shows a residual in a distorted tetrahedral extra-framework cavity which is suitable for Be. In the structural model for hellandite, this cavity hosts the H atoms bonded to O5; however, significant F is present in hellandite from Capranica, and the structure refinement shows that F occurs at O5. SIMS analyses also suggest the presence of some Li (0.49 apfu), which could be assigned to all the available cationic sites in the structure. However the following observations suggest that Li does not occur at the sixfold- and eightfold-coordinated sites: (1) the recalculated formula has cation sums already beyond the stoichiometric limit; (2) the observed <M1-O> distance, which is not compatible with a large cation such as $^{[6]}$Li; (3) comparison of the refined site-scatterings with those calculated from the unit formula excludes low-Z elements at sites M1-M4 but is consistent with additional occupancy at the Be site; and (4) crystal-chemical substitutions generally involve the lowest possible changes in the ionic charge in each site. We thus suggest

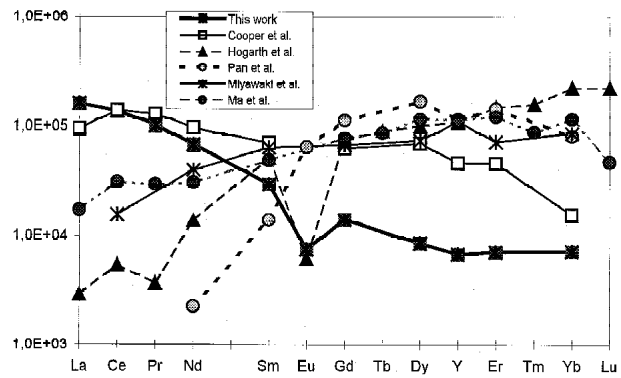

FIGURE 2. The different chondrite-normalized REE patterns available for hellandite from the literature. These do not show any selectivity towards incorporation of REE, their proportions being probably ruled by the paragenesis and the geological history of the rock.

that Li occurs in tetrahedral coordination in hellandite and enters the extra-framework site. If this is the case, we have at least 1.47 apfu (from SIMS; something more from the structure refinement) at Be, to be summed with 1.02 H apfu bonded to O5. Thus the distorted tetrahedral cavity located within Si1Si2Si2 trimers (Fig. 1) is occupied alternatively by Be (and/or Li), H (in a slightly different position), and might also be vacant.

Table 3 shows that the Be tetrahedron is a very distorted pseudo-trigonal pyramid with the O3, O10, and O11 O atoms at the basis and flattened along the apical Be-O5 direction. The basal Be-O3, Be-O10, and Be-O11 distances are ~0.20 Å longer than those usually reported as an average <$^{[4]}$Be-O>. Also, the Be-(O,F)5 distance is only slightly longer than expected on the basis of the Be and O ionic radii, but longer than expected for Be and F. The displacement parameters of the three basal O atoms (which are shared with the Si tetrahedra and with the M-sheet), are far larger than those of the other O atoms in the structure, and that of the Be site are larger than those of the other cationic sites (Table 2, Fig. 3a); the calculated shifts along the maximum components of the atomic displacement parameters are 0.32, 0.36, and 0.36 Å, respectively, for O3, O10, and O11. All these features indicate the presence of a larger cation (0.59 Å for Li vs. 0.27 Å for Be; Shannon 1976) and consequently positional disorder. We must also consider that the image given by the structure refinement is an average throughout the crystal of locally different arrangements involving Be, Li, H (±□) in the extra-framework cavity. The orientation of the atomic displacement parameters (Fig. 3a) agrees with the presence of positional disorder.

The atomic displacement parameter observed for O5 are within the expected ranges; the O5 anion site is occupied by F or O and is bonded only to M1; therefore, it does not suffer from the complex substitutions (in terms of both ionic radii and cationic charge) occurring at the eightfold-coordinated sites. The opposite reasoning can also explain the higher distortion parameters (Table 3) observed for the Si2 tetrahedron (which is connected with two Be sites) with respect to Si1.

The Si and B sites in hellandite from Capranica (1.636, 1.626, 1.495, and 1.487 Å, respectively) are larger than in the sample of Cooper et al. (1998) (1.623, 1.614, 1.498, and 1.486) and smaller than in that from Predazzo (1.641, 1.626, 1.512, and 1.507 Å; Mellini and Merlino 1977). The distortion of the B1 and B2 tetrahedra is higher in our sample and in that of Cooper et al. (1998) than in Mellini and Merlino (1977). The observed <B-O> distances fall within the range reported in the literature (1.462–1.512 Å, according to Hawthorne et al. 1996), and in the former two cases correspond to low fractional s-character of the (sp^3-hybrid) bond (Zhang et al. 1985). Concerning tetrahedral distortion, in hellandite from Capranica the distances with the apical O atoms (B1-O7 and B2-O6) are 0.07 Å shorter than B1-O13 and B2-O12 (the O atoms connecting two B tetrahedra) and 0.14 Å shorter than the other two B-O distances. All the basal edges of the B tetrahedra are shared with the large M2, M3, and M4 sites.

Short-range and long-range ordering in hellandite

If Be/Li and H alternate in the tetrahedral cavity on the two sides of the M1 octahedra, the center of symmetry would locally disappear. This situation would probably extend to the whole M-sheet because of charge-balance considerations. If this short-range order were present also at the long-range level (throughout the crystal), the symmetry would be lowered from the *P*2/*a* to the *P*2 space group. Around 15 out of the 300 reflections of the type *h*0*l* with $h = 2n + 1$ have intensities above the 5 $\sigma(I)$ level. However, they were not enough to allow refinement of the data in the *P*2 space group. Infrared spectroscopy could help to clarify the presence of local order.

Both refined site-scatterings and SIMS analyses suggest that Be and Li are locally associated to F, forming a BeO_3F tetrahedron; within the limit of the accuracy in elemental concentrations, the recalculated formula (Table 6) is compatible with dehydrogenation of O5, which should also be locally associated with Be and Li.

The refined site-scatterings confirm a site preference M2 >> M4 > M3 for (REE + actinides), in agreement with Mellini and Merlino (1977); in particular actinides and HREE are most likely to enter only the M2 sites.

In contrast to the results of Cooper et al. (1998), no significant disorder of the REE at M2 was observed in the non-metamict hellandite from Capranica. The displacement

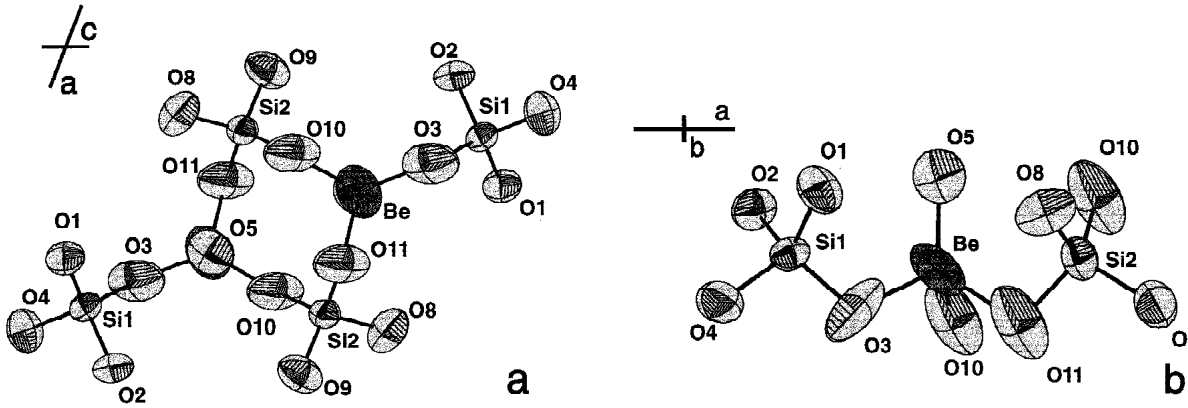

FIGURE 3. The coordination of the partially occupied Be site, with atomic displacement ellipsoids for the relevant atoms. **(a)** Projections along [010]. **(b)** Along [001].

TABLE 6. Chemical composition

oxide	wt%	atom	apfu
SiO_2	22.776	Si	8.11
B_2O_3	12.986	B	7.98
BeO	1.141	Be	0.98
Li_2O	0.340	Li	0.49
TiO_2	1.518	ST	17.55
Al_2O_3	1.967	Ti	0.41
Fe_2O_3	2.445	Al	0.83
Mn_2O_3	0.202	Fe^{3+}	0.65
Cr_2O_3	0.010	Mn^{3+}	0.02
MgO	0.247	Mg	0.13
BaO	0.002	ÂM1	2.04
CaO	21.518	Ca	8.21
ThO_2	9.516	Th	0.77
UO_2	1.400	U	0.11
Y_2O_3	1.345	Y	0.25
La_2O_3	4.510	La	0.59
Ce_2O_3	10.010	Ce	1.30
Pr_2O_3	1.125	Pr	0.15
Nd_2O_3	3.655	Nd	0.46
Sm_2O_3	0.510	Sm	0.06
Eu_2O_3	0.049	Eu	0.01
Gd_2O_3	0.319	Gd	0.04
Dy_2O_3	0.240	Dy	0.03
Er_2O_3	0.129	Er	0.01
Yb_2O_3	0.133	Yb	0.01
F	0.870	SM2,3,4	12.01
H_2O	0.430	OH	1.02
O=F	0.370	F	0.98
Total	99.03	O^{2-}	2.00
		ÂO5	4.00

Notes: Unit-formula recalculation on the basis of 48 (O + F). Σ indicates summation of the preceeding entries.

parameter of the M2 site is the smallest among the eightfold-coordinated sites. This different behavior might also be related with the ionic radii of Th and U being smaller than those of the LREE and closer to those of Y and HREE. However, all the atomic displacement parameters of the cationic and anionic sites have one component (β_{22}) systematically larger than the others. This fact is consistent with some positional disorder along the direction of the *b* axis, in stringent analogy with what already discussed for the Be site.

Variations of the unit-cell parameters within the hellandite group

Comparison of all the available data for hellandite and tadzhikite shows that the unit-cell parameters regularly increase as a function of the Ca content (Fig. 4), the most sensitive parameters being the *a* edge, as suggested by Hogarth et al. (1972). Use of CaO as the independent variable gives better relationships than those using Ca apfu, suggesting incomplete chemical analysis and problems in the formula recalculation concerning water content. The unit-cell dimensions of hellandite from Capranica fall within the observed trends, suggesting that the presence of cations at the extra-framework site either does not affect the hellandite structure or is more ubiquitous than expected. Significant deviations (in the sense of longer unit-cell edges or of lower Ca contents than expected) are observed for the sample of Cooper et al. (1998).

Relationships with other structures

The present structure refinement shows that at least under high activity of F, Be, and Li in the system, the only cavity available in the hellandite structure that is usually occupied by

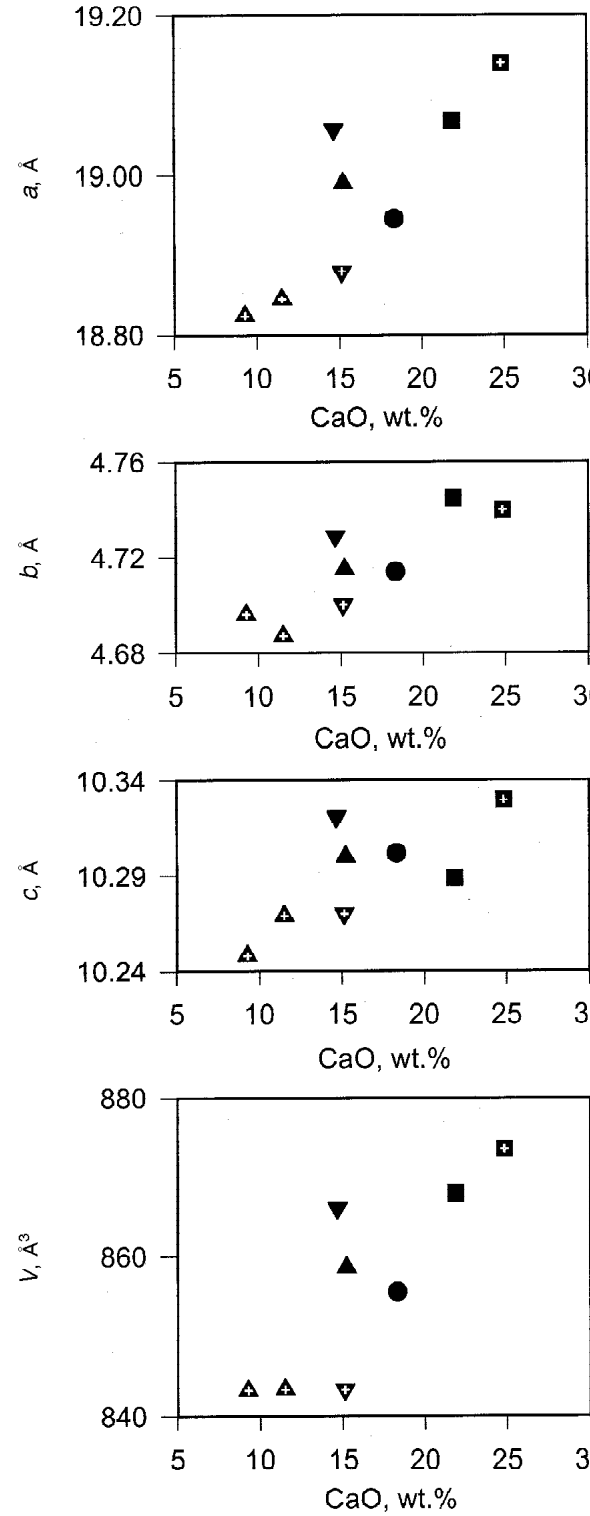

FIGURE 4. Unit-cell parameters vs. CaO content in hellandite. Black square = this work; black upward triangle = Mellini and Merlino 1977; black downward triangle = Cooper et al. 1998; black circle = Chernitsova et al. 1972; crossed square = Mt. Cavalluccio (Italy), CSCC unpublished results; crossed upward triangles = Hogarth et al. 1972; crossed downward triangle = Pan et al. 1994.

H can be filled with Be and/or Li in tetrahedral coordination. When this is the case, the $[B_4Si_4O_{22}]$ chains are connected into a continuous two-dimensional tetrahedral sheet composed of four-, five- and eight-membered rings. These rings are of the types Be_2Si2_2, $BeB2_2Si1Si2$, $B1_2B2Si1Si2$, and $Be_2B1_2Si1_2Si2_2$, respectively (Fig. 5). The tetrahedral sheets alternate with sheets composed of M1 octahedra occupied by trivalent (Al, Fe) and tetravalent Ti cations and by eightfold-coordinated M2, M3, and M4 square antiprisms occupied by Ca, REE, and actinides in variable proportions.

Mellini and Merlino (1977) proposed analogies between hellandite and the melilite-group minerals like meliphanite, Ca(Ca,Na) $BeSi_2O_6F$ (Dal Negro et al. 1967), leucophanite, and REE-bearing leucophanite, (Ca,REE) $CaNa_2Be_2Si_4O_{12}(F,O)_2$ (Cannillo et al. 1992), in which the tetrahedral sheet consists of five-membered rings of SiO_4 and BeO_3F tetrahedra. Their analogy is corroborated by the discovery of the BeO_3F tetrahedron, which makes hellandite a sheet mineral in the classification of Zoltai (1960). More stringent analogies can be found with semenovite $[REE_2Na_{0-2}(Ca,Na)_8(Fe^{2+},Mn,Zn,Ti)(Si,Be)_{20}(O,OH,F)_{48}]$ (Mazzi et al. 1979) and nordite $[(La_{2.1}Ce_{1.7}Ca_{0.2})(Sr_{2.1}Ca_{1.9})Na_2(Na_{0.8}Mn_{0.2})(Zn_{1.5}Mg_{1.3}Fe^{2+}_{0.7}Mn_{0.5})(Si_{5.85}Fe^{3+}_{0.15})O_{17}$; Bakakin et al. 1970). In semenovite, sheets built up with four-, five- and eight-membered rings of (Si, Be) tetrahedra alternate, even if with a different arrangement, with sheets of four independent (Ca,Na,REE) eightfold-coordinated polyhedra and two independent (Fe,Mn) octahedra. In nordite, sheets of four-, five-, and eight-membered rings of Si tetrahedra alternates with sheets made by three independent (Na), (Ca,Sr) and (Ca,REE) eightfold-coordinated polyhedra and by two independent (Mn,Na) and (Zn,Mg,Fe,Mn) octahedra. Mazzi et al. (1979) noticed the structural analogy with semenovite if a vacant tetrahedral site is filled in hellandite.

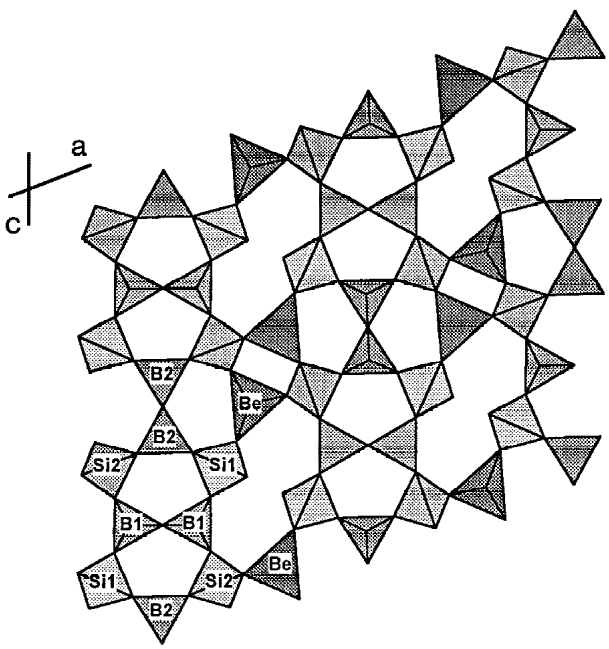

FIGURE 5. The tetrahedral sheet of hellandite in the case of complete occupancy (4 apfu) of the extra-framework Be site.

CONCLUSIONS

The present study provides answers to the questions on the hellandite crystal-chemistry given in the introduction paragraph. (1) As suggested in previous papers (Mellini and Merlino 1977; Chernitsova et al. 1982), hellandite and tadzhikite are isostructural and can be considered as members of the same mineral group. However, the tetrahedral layer of hellandite-group minerals contains an extra-framework tetrahedral cavity which, at least under particular conditions, can host $^{[4]}$Be and/or $^{[4]}$Li. When this is the case, hellandite is better described as a sheet-like borosilicate. (2) Although particular care was used to check the surroundings of the O6 and O7 atoms, no residual suitable for H has been found in the difference Fourier map beyond the one near O5. This is in good agreement with the H content obtained by SIMS. Also, no vacancy is observed for the studied hellandite, in which nearly all the REE and the actinides elements were analyzed by SIMS. On the basis of our results, we propose that the structural formula $(Ca,REE)_8(Th,U,Y,REE)_4(Ti,Fe^{3+},Al)_2(O,F,OHx)_4(Be,Li)_{4-x}Si_8B_8O_{44}$ is valid for both hellandite and tadzhikite. In this formula, the amount of H at O5 is constrained by the amount of $^{[4]}$Be and $^{[4]}$Li at the extra-framework site, and the overall electroneutrality is maintained by an appropriate combination of heterovalent substituents at the M sites. (3) The major differences within the hellandite-group minerals are related to the chemistry of the M-layer. The M1 octahedra are occupied mainly by Al and Fe^{3+}, but crystals rich in Ti^{4+} have been also described. The M1 cations bond to the O5 anion; therefore high Ti^{4+} contents at M1 may also compensate for the lack of H at O5. However, the most important compositional variations are related to the substituents at the M2, M3, and M4 eightfold-coordinated polyhedra, in which variable proportions of Ca, lanthanides and actinides can occur. For this reason we propose that hellandite-group minerals should be named according to the rule of Levinson (1966) which states that REE-bearing minerals should be classified not with end-member names, but using a combination of a structural formula name plus a symbol for the dominant lanthanide element. Therefore, the sample from Capranica, like tadzhikite, should be named hellandite-(Ce), those from Mattagami Lake, China, and Japan as hellandite-(Y), that from Predazzo as hellandite-(Gd), those from Norway and Wakefield Lake as hellandite-(Yb), etc. (4) It should be finally noted that the dimensions of the tetrahedral sheet in these minerals are constant because of its constant composition, thus the possibility of incorporating larger elements at the eightfold-coordinated sites is controlled mainly by the composition of the M1 site, i.e., increasing Fe^{3+} at M1 should allow for the entrance in the structure of LREE.

ACKNOWLEDGMENTS

Financial supports to F.C. from a FPU research grant of the Spanish MEC, and to G.D.V. from the Accademia dei Lincei-Commissione per i Musei naturalistici e Musei della Scienza, and to the EMP laboratory of the Università di Modena from the CNR are gratefully acknowledged.

REFERENCES CITED

Anders, E. and Ebihara, M. (1982) Solar System abundances of the elements. Geochimica et Cosmochimica Acta, 46, 2363–2380.

Anovitz, L.M. and Hemingway, B.S. (1996) Thermodynamics of boron minerals: summary of structural, volumetric and thermochemical data. In Mineralogical

Society of America Reviews in Mineralogy, 33, 181–262.
Armstrong, J.T. (1988) Quantitative analysis of silicate and oxide minerals. Comparison of Monte-Carlo, ZAF and Phi-Rho-Z procedures. Microbeam Analyses, 239–246.
Bakakin, V.V., Belov, N.V., Borisov, S.V., and Solovyeva, L.P. (1970) The crystal structure of nordite and its relationship to melilite and datolite-gadolinite. American Mineralogist, 55, 1167–1181.
Bottazzi, P., Ottolini, L., Vannucci, R., and Zanetti, A. (1994) An accurate procedure for the quantification of rare earth elements in silicates. A. Benninghoven, Y. Nihei, R. Shimizu and H.W. Werner, Eds., SIMS IX Proceedings, p. 927–930. Wiley, Chichester, U.K.
Brögger, W.C. (1922) Hellandit. Vid. Selsk. Sk. (Oslo). Mat-Nature KI, 6, 1–16.
Cannillo, E., Giuseppetti, G., Mazzi, F., and Tazzoli, V. (1992) The crystal structure of a rare earth bearing leucophanite, $(Ca,RE)CaNa_2Be_2Si_4O_{12}(F,O)_2$. Zeitschrift für Kristallographie, 202, 71–79.
Chernitsova, N.M., Pudovkina, Z.V., and Pyatenko, Y.A. (1982) About the crystal structure of tadzhikite $(CaTr)_4(Y,Tr)_2(Ti,Fe,Al)(O,OH)_2(Si_4B_4O_{22})$. Doklady Akademii Nauk SSSR, 264, 342–344.
Cooper, M.A., Hawthorne, F.C., and Taylor, M.C. (1998) Refinement of the crystal structure of tadzhikite. Canadian Mineralogist, 36, 817–827.
Dal Negro, A., Rossi G., and Ungaretti, L. (1967) The crystal structure of meliphanite. Acta Crystallographica, 23, 260–264.
Donovan, J.J. and Rivers, M.L. (1990) PRSUPR—A PC based automation and analysis software package for wavelength-dispersive electron-beam microanalysis. Microbeam Analysis, 25, 66–68.
Drake, M.J. and Weill, D.F. (1972) New rare earth element standards for electron microprobe analysis. Chemical Geology, 10, 179–181.
Emiliani, F. and Gandolfi, G. (1965) The accessory minerals from Predazzo granite (North Italy). Part III (datolite, gadolinite, hellandite, ancylite, synchisite, uraninite). Mineralogica Petrografica Acta, 11, 123–131.
Hawthorne, F.C., Burns, P.C., and Grice, J.D. (1996) The crystal chemistry of boron. In Mineralogical Society of America Reviews in Mineralogy, 33, 41–116.
Hawthorne, F.C., Ungaretti, L., and Oberti, R. (1995a) Site populations in minerals: terminology and presentation of results of crystal-structure refinement. European Journal of Mineralogy, 33, 907–911.
Hawthorne, F.C., Cooper, M., Bottazzi, P., Ottolini, L., Ezcit, S.T., and Grew, E.S. (1995b) Micro-analysis of minerals for boron by SREF, SIMS and EMPA: a comparative study. Canadian Mineralogist, 33, 389–397.
Hinton, R.W. (1990) Ion microprobe trace-element analysis of silicates: Measurement of multi-element glasses. Chemical Geology, 83, 11–25.
Hogarth, D.D., Chao, G.Y., and Harris, D.C. (1972) New data on hellandite. Canadian Mineralogist, 11, 760–776.
Lehman, M.S. and Larsen, F.K. (1974) A method for location of the peaks in step-scan measured Bragg reflection. Acta Crystallographica, A30, 580–586.
Levinson, A.A. (1966) A system of nomenclature for rare-earth minerals. American Mineralogist, 51, 152–158.
Locardi, E. (1965) Tipi di ignimbriti di magmi mediterranei: il vulcano di Vico. Atti Società. Toscana Scienze Naturali, 45, 55–173.
Ma, Z., Zhang, J., and Yang, F. (1986) Hellandite of Quyang, Hebei, China. Dizhi Xuebao, 60, 68–77.
Mazzi, F., Ungaretti, L., Dal Negro, A., Petersen, O.V., and Rönsbo, J.G. (1979) The crystal structure of semenovite. American Mineralogist, 64, 202–210.
Mellini, M. and Merlino, S. (1977) Hellandite: a new type of silicoborate chain. American Mineralogist, 62, 89–99.
Miyawaki, R., Nakai, I., Nagashima, K., Okamoto, A., and Isobe, T. (1987) The first occurrence of hingganite, hellandite and woodginite in Japan. Kobutsugaku Zasshi, 18, 17–30.
North, A.C.T., Phillips, D.C., and Mathews, F.S. (1968) A semi-empirical method of absorption correction. Acta Crystallografica, A24, 351–359.
Oftedal, I. (1965) Uber den Hellandit. Tschermaks Mineralogisch- Petrographische Mitteilungen, 10, 125–129.
Ottolini, L., Bottazzi, P., and Vannucci, R. (1993) Quantification of lithium, beryllium and boron in silicates by Secondary Ion Mass Spectrometry using conventional energy filtering. Analytical Chemistry, 65, 1960–1968.
Ottolini, L., Bottazzi, P., and Zanetti, A. (1994) Quantitative analysis of hydrogen, fluorine and chlorine in silicates using energy filtering. A. Benninghoven, Y. Nihei, R. Shimizu and H.W. Werner, Eds., SIMS IX Proceedings, p. 191–194. Wiley, Chichester, U.K.
Ottolini, L., Bottazzi, P., Zanetti, A., and Vannucci, R. (1995) Determination of H in silicates by Secondary Ion Mass Spectrometry, Analyst, 120, 1309–1313.
Pan, Y., Fleet, M.E., and Barnett, R.L. (1994) Rare-earth mineralogy and geochemistry of the Mattagami Lake volcanogenic massive sulfide deposit, Quebec. Canadian Mineralogist, 32, 33–147.
Reed, S.J.B. (1985) Ion-probe determination of rare earths in allanite. Chemical Geology, 48, 137–143.
Shannon, R.D. (1976) Revised effective ionic radii and systematic studies of interatomic distances in halides and chalcogenides. Acta Crystallographica, A32, 751–767.
Yefimov, A.F., Dusmatov, V.D., Alkhazov, V.Yu., Pudovkina, Z.G., and Kazakova, M.Y. (1970) Tadzhikite, a new rare-earth borosilicate of the hellandite group. Doklady Akademii Nauk SSSR, 195, 136–139.
Zhang, Z.G., Boisen, M.B. Jr., Finger, L.W., and Gibbs, G.V. (1985) Molecular mimicry of the geometry and charge density distribution of polyanions in borate minerals. American Mineralogist, 70, 1238–1247.
Zoltai, T. (1960) Classification of silicates and other minerals with tetrahedral structures. American Mineralogist, 45, 960–973.

MANUSCRIPT RECEIVED MARCH 9, 1998
MANUSCRIPT ACCEPTED NOVEMBER 19, 1998
PAPER HANDLED BY LEE A. GROAT